Influence of thermal balance on cold-induced vasodilation

Andreas D. Flouris[1] and Stephen S. Cheung[1,2]

[1]*Environmental Ergonomics Laboratory, School of Health and Human Performance, Dalhousie University, Halifax, Nova Scotia; and* [2]*Department of Physical Education and Kinesiology, Brock University, St. Catharines, Ontario, Canada*

Flouris AD, Cheung SS. Influence of thermal balance on cold-induced vasodilation. *J Appl Physiol* 106: 1264–1271, 2009. First published February 12, 2009; doi:10.1152/japplphysiol.91426.2008.—We examined the effect of thermal balance perturbation on cold-induced vasodilation through a dynamic A-B-A-B design applying heat (*condition A*) and cold (*condition B*) to the body's core, while the hand is exposed to a stable cold stimulus. Fifteen healthy adults (8 men, 7 women) volunteered. Applications of heat and cold were achieved through water immersions in two tanks maintained at 42 and 12°C water temperature, respectively, in an A-B-A-B fashion. Throughout the experiment, the participants' right hand up to the ulnar styloid process was placed inside a temperature-controlled box set at 0°C air temperature. Results demonstrated that cold-induced vasodilation occurred only during *condition B* and at times when body heat content was decreasing but rectal temperature had not yet dropped to baseline levels. Following the occurrence of all cold-induced vasodilation events, rectal temperature was reduced, and the phenomenon ceased when rectal temperature fell below baseline. Heart rate variability data obtained before and during cold-induced vasodilation demonstrated a shift of autonomic interaction toward parasympathetic dominance, which, however, was attributed to a sympathetic withdrawal. Receiver operating characteristics curve analyses demonstrated that the cold-induced vasodilation onset cutoff points for rectal temperature change and finger temperature were 0.62 and 16.76°C, respectively. It is concluded that cold-induced vasodilation is a centrally originating phenomenon caused by sympathetic vasoconstrictor withdrawal. It is dependent on excess heat, and it may be triggered by excess heat with the purpose of preserving thermal balance.

finger blood flow; thermoregulation

COLD-INDUCED VASODILATION (CIVD) is a counterintuitive acute increase in local cutaneous blood flow occurring in humans and other homoeotherms exposed to cold (11), first identified in 1930 (35). The emergence of CIVD has been described as nonsystematic, and, hence, its function(s) as well as its causative agent(s) remain unexplainable (10, 11, 40). We recently proposed that CIVD is a thermoregulatory mechanism triggered by increased mean body temperature (19). Although our finding was based on finger temperature and not on actual blood flow data, it is supported by observations of a central component to CIVD (8, 34, 37, 41, 42, 46). Furthermore, thermal balance has been shown to influence CIVD in a way that whole body cooling results in delayed CIVD onset (14, 17, 30, 46), whereas increased thermogenesis (44) or body heat content (14) result in accelerated CIVD response.

The difficulty to hitherto elucidate the CIVD response may be partly attributable to the currently incomplete understanding of its neurophysiological mechanisms. These mechanisms can be explored by monitoring heart rate variability (HRV) during CIVD because the cardiovascular adaptations to thermal stimuli are the result of a simultaneous activation of the peripheral vascular and cardiac efferent branches of the autonomic nervous system (36).

Our primary objective in this experiment was to collect blood flow data for the effect of thermal balance perturbation on CIVD through a dynamic A-B-A-B design applying heat (*condition A*) and cold (*condition B*) to the body's core, while the hand is exposed to a stable cold stimulus. The A-B-A-B design is one of the most widely adopted designs to examine the causal effects of an intervention, as well as the causal relationships, between target responses and causal variables (28). Based on our recent finding that CIVD is triggered by increased body temperature (19), we hypothesized that CIVD would be evident only when excess heat would be present. Our secondary objective in this experiment was to develop a HRV-based neurophysiological characterization of CIVD. Based on previous findings showing a central component to CIVD, we hypothesized that HRV data collected during CIVD would be significantly different from those collected when CIVD was absent.

METHODS

Participants and procedures. The experimental protocol conformed to the standards set by the Declaration of Helsinki and was approved by the appropriate ethical review board at Dalhousie University. Eight male and seven female nonsmoking adults (age: 24.9 ± 4.6 yr; body mass index: 24.9 ± 4.3; body fat: $16.3 \pm 9.2\%$; body surface area: 1.9 ± 0.2 m²; means $\pm$ SD) volunteered for the study. Participants were screened for Raynauld's phenomenon and medications for high blood pressure. Female subjects were screened for pregnancy and tested during the early follicular phase (*days 1–6*) of their menstrual cycle. Written, informed consent was obtained from all participants after full explanation of the procedures involved. Participants were given a detailed verbal description of the protocol, followed by extensive familiarization with all data collection procedures and instruments during an initial familiarization session performed at least 3 days before testing. Anthropometrical measurements were also performed at this time.

Before data collection, participants dressed down to a bathing suit; male participants wore a regular one-piece swimming suit, while female participants wore either a one (full)- or a two-piece swimming suit. Throughout data collection, the participants' right hand up to the ulnar styloid process was placed inside a temperature-controlled box set at 0°C air temperature. Following a 15-min baseline period, participants entered a water tank maintained at 42°C water temperature and passively rested until their rectal temperature (T_{re}) was raised by 0.5°C above baseline. Thereafter, they exited the warm bath and entered a different water tank maintained at 12°C water temperature until their T_{re} was decreased by 0.5°C below baseline. This procedure

was repeated twice. No certain timeframe was set, as the objective of the protocol was to reach a certain increase or decrease in T_{re}. During baseline, participants relaxed in a semisupine position, while during water immersion they remained in the same position and were immersed up to the upper part of their chest, slightly below the level of the clavicle. Their arms during baseline and water immersion were supported at the level of the heart, with the right hand placed inside the temperature-controlled box, and were not immersed in the water at any time.

The baseline measurements were conducted with participants relaxed, seated in a ventilated and air-conditioned thermoneutral environment (ambient temperature: 25°C; relative humidity: 40%) for 15 min. During this time, their upper body was partly covered with a light blanket to minimize heat loss due to lack of clothing. Testing was conducted by the same investigators and between 0900 and 1400. Participants were instructed to consume a light breakfast and adequate amounts of water before arriving in the laboratory, having abstained from alcohol and caffeine for 12 h. Ad libitum water ingestion was permitted during data collection. Participants were also advised to avoid physical activity and excessive stressors, such as exposure to extreme hot or cold temperatures for 48 h before data collection and particularly during the period between awakening and experimentation and during transit from home to the laboratory.

Finger blood flow (BF_F) was measured using laser-Doppler velocimetry (PeriFlux System 5000, main control unit; PF5010 LDPM, function unit; Perimed, Stockholm, Sweden) at the pulp of the right-hand index finger. A calibration device (PF 1000, Perimed) standard was used to adjust the laser-Doppler flowmeter readings to coincide with the readings obtained with Perimed's Motility Standard. The probe (PR 407 small straight probe, Perimed) was held in place with a plastic mini holder (diameter: 5 mm; PH 07-5, Perimed), which was fixed to the skin using double-sided adhesive strips (PF 105-3, Perimed) without constricting the finger. BF_F was expressed in perfusion units and was sampled at 32 Hz. These data were then used to provide 1-min mean BF_F values.

To assess T_{re}, participants self-inserted a flexible T_{re} probe [2 mm in diameter (Mon-A-Therm Core, Mallinckrodt Medical, St. Louis, MO)] to a depth of 15 cm beyond the anal sphincter. A flexible thermistor (MA-100, Thermometrics, Edison, NJ) was inserted in the participants' ear canal and was used as an index of tympanic temperature (T_{ty}). The probe was pushed gently until such a time as it touched the tympanic membrane. At this point, the participant sensed a slight discomfort, and the probe was then retracted slightly. The probe was secured in its position by packing the ear with cotton balls held in place with surgical tape (3M Transpore Tape, 3M Canada). Two ceramic chip skin thermistors (MA-100, Thermometrics) were attached on the pad's lower part (below the Doppler probe mini holder) on the second (i.e., index) and on the pad of the fourth (i.e., ring) finger of the right hand (i.e., the hand placed inside the temperature-controlled box) with surgical tape (3M Transpore Tape, 3M Canada) to allow the measurement of finger temperature (i.e., mean of the two fingers, T_f). Values for T_{re}, T_{ty}, and T_f were recorded throughout baseline and water immersion at 8-s intervals using a data logger (Smartreader 8 Plus, ACR, Vancouver, Canada) interfaced with a computer to allow for their continuous monitoring by the investigators. These values were used to provide 1-min mean values for each variable.

The change in body heat content (ΔH_b, in kJ) was calculated through the rate of body heat storage ($\dot{S}$) as the ΔH_b at time t (in min) from the initial H_b at 0 min based on the following procedure.

The $\dot{S}$ was calculated based on standardized procedures (39) as:

$$\dot{S} = \dot{M} - \dot{W} - \dot{E}_{res} - \dot{C}_{res} - \dot{E}_{sk} - (\dot{K} + \dot{C} + \dot{R})$$

where all variables are measured in watts (W) and $\dot{M}$ is the metabolic rate; $\dot{W}$ is the rate of work; $\dot{E}_{res}$ and $\dot{C}_{res}$ are the rates of evaporative and dry (convective) heat flow through the respiratory tract, respectively; $\dot{E}_{sk}$ is the evaporative heat flow from the skin, and $\dot{K}$, $\dot{C}$, and

$\dot{R}$ represent the conductive, convective, and radiative heat flows from the skin, respectively.

$\dot{M}$ was assessed via open-circuit spirometry using an automated gas analyzer indirect calorimetry system (TrueOne 2400, Parvo Medics, Sandy, UT). Breath-by-breath respiratory parameters were recorded and were expressed in 15-s averages while participants inspired room air through a mask. The gas analyzer was calibrated with standard gases before testing. $\dot{M}$ was determined using a validated formula (21):

$$\dot{M} = [(0.23 \cdot RQ + 0.77) \cdot 21.14] \cdot (60 \cdot \dot{V}_{O_2}) \cdot A_D$$

where $(0.23 \cdot RQ + 0.77) \cdot 21.14$ represents the energy equivalent of oxygen consumed (in kJ/l), RQ is the respiratory quotient, $\dot{V}_{O_2}$ is the oxygen uptake (in l/min in standard temperature and pressure, dry), and A_D is the body surface area (15).

$\dot{W}$ was equal to 0 W, as participants were resting throughout the experiment. Based on validated procedures (18), $\dot{E}_{res}$ and $\dot{C}_{res}$ were calculated using $\dot{M}$, while assuming an upper respiratory tract mean temperature of ~37°C and corresponding saturated vapor pressure of ~6.51 kPa. Since ~93% of the body was immersed in water, $\dot{E}_{sk}$ was not assumed to be significantly different from zero and was thus not measured. Furthermore, due to the limited direct contact between the body and external solid objects in the current experiment, the contribution of $\dot{K}$ in calculating $\dot{S}$ was assumed to be negligible, as previously suggested (3).

Measurement of ($\dot{C} + \dot{R}$) was achieved using 12 calibrated heat flux transducers with embedded thermistors (FR-025-TH44033-F6, Concept Engineering, Old Saybrook, CT), which were attached to the skin according to a widely used skin temperature model (27) with heat flux (including the head) calculated as follows: 0.07 forehead + 0.14 arm + 0.05 hand + 0.07 foot + 0.13 (shin + calf)/2 + 0.19 (quadriceps + hamstrings)/2 + 0.35 (chest + abdomen + upper back + lower back)/4. All heat flux transducers were held in place against the skin with surgical tape (3M Transpore Tape, 3M Canada) covering the neoprene edges of custom-made holders for each transducer so that the disk itself was left uncovered. Values for heat flow were recorded and displayed throughout the thermal protocol at 1.5-s intervals using data-acquisition software (EasyDaq, Dorset, UK). Thereafter, these values were used to provide 1-min mean values for each variable.

To complete the calculation of ΔH_b, minute-by-minute $\dot{S}$ data, expressed in watts, were converted to kilojoules per minute using the formula:

$$\dot{S}(kJ/min) = \frac{\dot{S}(W) \cdot 60}{1,000}$$

The ΔH_b from 1 min to the next was calculated [except at $t = 0$ min, where ΔH_b (kJ) = $\dot{S}_0$ (kJ)] as follows:

$$\Delta H_{bt} = \Delta H_{bt-1} + \dot{S}_t$$

These data were subsequently normalized so that $\Delta H_{b0} = 0$, while ΔH_b over the course of the experiment was tracked using the formula:

$$\Delta H_b = \Delta H_{bt} - \Delta H_{b0}$$

To assess autonomic modulation, participants were outfitted with a heart rate chest strap, and HRV data were sampled through short-range telemetry at 1,000 Hz with a Polar S810 (Kempele, Finland), a device validated for HRV measurements (22). The heart rate monitor signal was transferred to the Polar Precision Performance Software (release 3.00; Polar Electro Oy), and R-R intervals were exported under ASCII format. Both frequency domain and time domain measures were analyzed using HRV analysis software version 1.1 (Finland; Biomedical Signal Analysis Group, Department of Applied Physics, University of Kuopio, Finland 2002). To assess frequency domain measures, the power spectra were estimated using a 1,024-point linear fast Fourier transform algorithm. The power spectra were then analyzed for total (0.0–0.4 Hz), low- (LF; 0.04–0.15 Hz), and

high-frequency (HF; 0.15–0.4 Hz) power. LF power reflects the mixed modulation of sympathetic and parasympathetic activities, whereas HF power is almost entirely mediated by parasympathetic activity in the sinoatrial node (1). We evaluated the R-R interval time series automatically obtained from the raw signals. From the R-R data, the square root of the mean of squared differences between successive intervals (RMSSD) was also computed, together with the percentage of the differences of successive normal-to-normal intervals >50 ms, normalized to all differences within the interval (pNN50),

LF, HF, as well as LF-to-HF ratio (LF/HF). The term "normal-to-normal intervals" refers to intervals between consecutive QRS complexes, resulting from sinus node depolarizations. To minimize influences on HRV values, participants were instructed to remain silent and as calm as possible throughout data collection.

Statistical analyses. Correlation coefficients were calculated among the time required to reach the core temperatures directed by the thermal protocol, body surface area, body fat percent, and body mass index. Thereafter, HRV data were divided in those obtained during
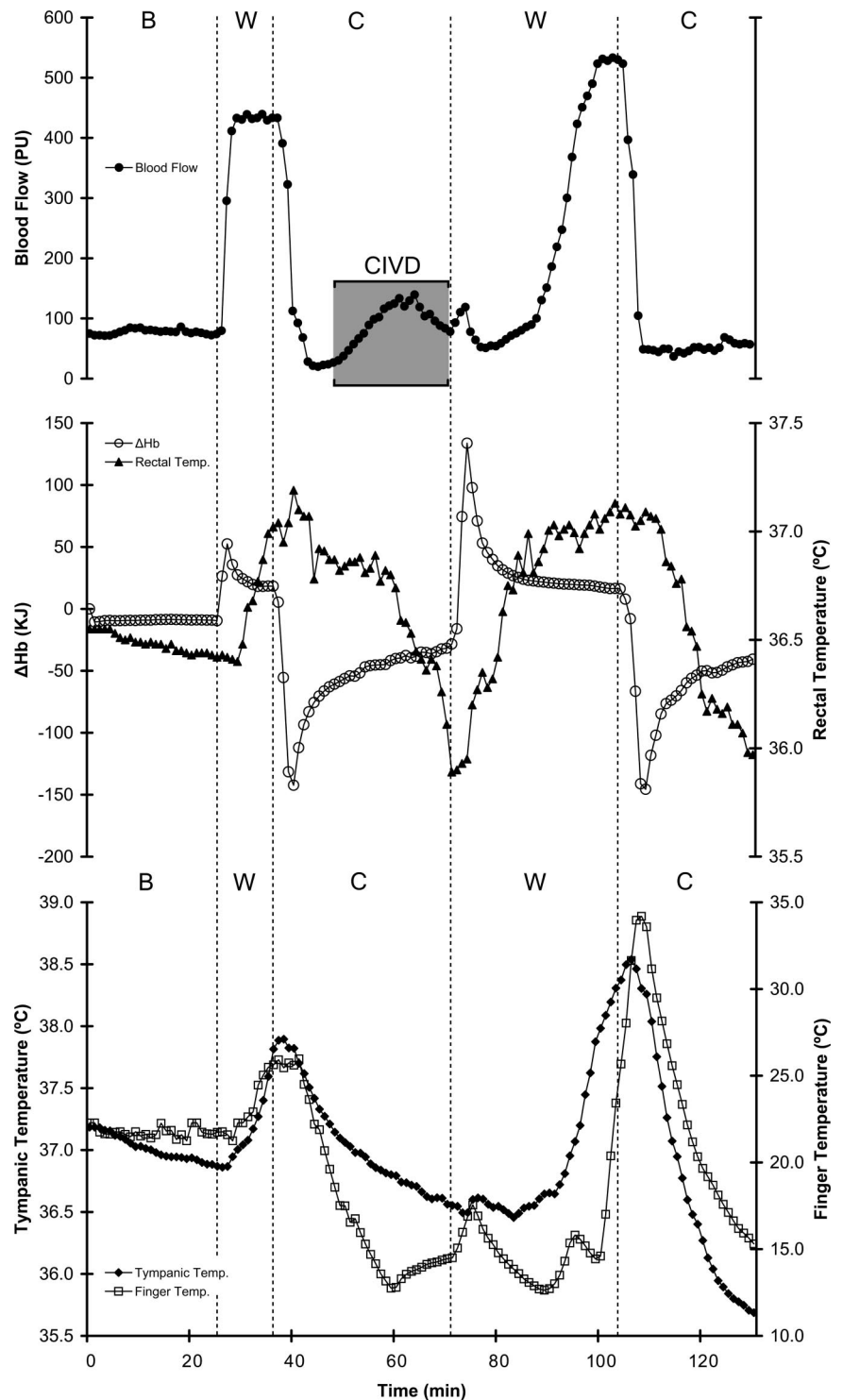

Fig. 1. Kinetics of finger blood flow (BF_F), change in body heat content (ΔH_b), rectal temperature (T_{re}), tympanic temperature (T_{ty}), and finger temperature (T_f) during baseline (B) as well as repetitive warming (W) and cooling (C) for a male participant chosen at random. PU, perfusion units; CIVD, cold-induced vasodilation.

hot and cold water immersion, χ^2 was used to detect differences in the occurrence of warming- and cooling-induced vasodilation, and repeated-measures ANOVA was used to detect differences in the duration as well as the change in T_{re}, BF_F, T_{ty}, and T_f between the onset and end of the two types of vasodilation. In addition, repeated-measures ANOVA followed by post hoc t-tests incorporating a Bonferroni adjustment were used to assess the effect of vasodilation segment (i.e., prewarming induced, during warming induced, precooling induced, during cooling induced) on all parameters of HRV (i.e., RMSSD, pNN50, LF, HF, as well as LF/HF), as well as on breath-by-breath respiratory data for respiratory rate (breaths/min), ventilation (l/min),

and tidal volume (liters) to address the well-known influence of ventilation on HRV (2). Pearson's correlation coefficients were further used to assess the relationships among HRV and ventilatory parameters across the different vasodilation segments.

Because of the difference in HRV found between cooling-induced and warming-induced vasodilation (see RESULTS), ΔT_{re} (change in T_{re} from baseline) and T_f data obtained only during cold water immersion were used in an attempt to detect possible CIVD thresholds for ΔT_{re} and T_f using receiver operating characteristics (ROC) curve analysis. Specifically, BF_F was transformed into a "dummy" dichotomous variable based on whether CIVD was present or absent. Thereafter,
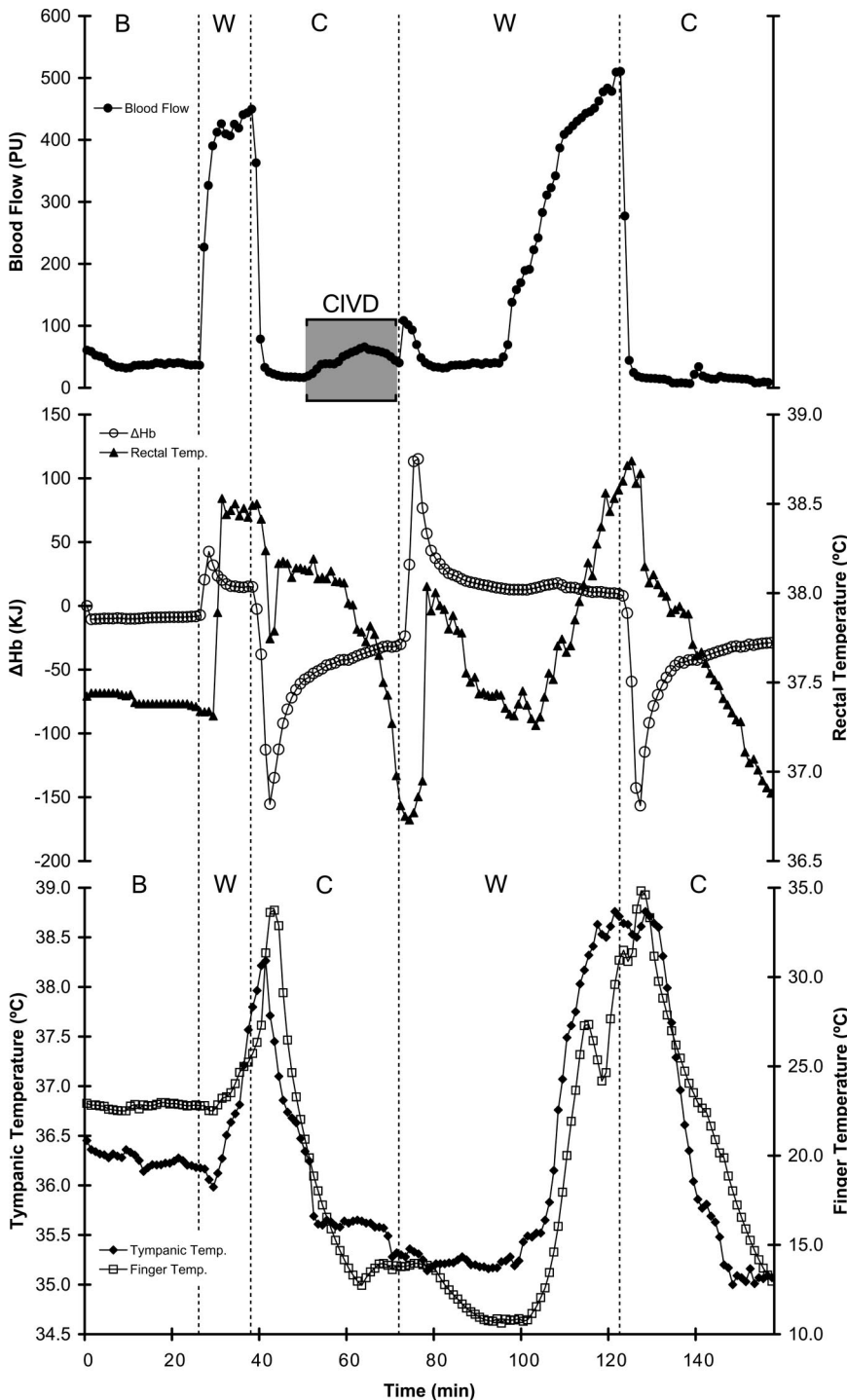

Fig. 2. Kinetics of BF_F, ΔH_b, T_{re}, T_{ty}, and T_f during B as well as repetitive W and C for a female participant chosen at random.

ROC curve procedures were applied on ΔT_{re} and T_f data in an attempt to detect possible thresholds for CIVD. The area under the ROC curve was estimated using the Wilcoxon nonparametric method (4). Calculated sensitivity and specificity with corresponding 95% confidence intervals were used to determine the efficacy of the two parameter (i.e., ΔT_{re} and T_f) cutoffs in detecting CIVD. Sensitivity was defined as the proportion of scores when CIVD was present that demonstrated a ΔT_{re} or T_f value indicating the presence of CIVD. Specificity was defined as the proportion of scores when CIVD was absent that revealed a ΔT_{re} or T_f value indicating absence of CIVD. Cohen's κ-statistic was used to evaluate the agreement between the ΔT_{re} and T_f cutoff values and the BF_F characterization. All statistical analyses were performed with SPSS (version 14.0.1, SPSS, Chicago, IL) statistical software package. The level of significance was set at $P <$ 0.05, except for post hoc tests in which a Bonferroni adjustment was applied.

RESULTS

Individual data are presented in Figs. 1 and 2 for BF_F, ΔH_b, T_{re}, T_{ty}, and T_f across time for one male and one female participant chosen at random. The patterns identified in these figures were observed in all 15 participants. The BF_F data demonstrated two characteristic patterns of vasodilation, depending on whether participants were immersed in hot or cold water. The warming-induced vasodilation occurred during the hot water immersion in circumstances in which T_{re} was either above baseline levels with an increasing trend or would soon increase past baseline, while the cooling-induced vasodilation occurred during the cold water immersion in cases in which T_{re} was above baseline levels but showed a declining trend. The warming-induced vasodilation resembled a typical vasodilatory response aiming at heat dissipation characterized by an initial rapid BF_F increase within 3–5 min followed by a plateau (38). The cooling-induced vasodilation occurred 5–10 min following cold water immersion and was characterized by a relatively small gradual increase in BF_F resembling what Lewis in 1930 described as CIVD (35). Thus henceforth, the cooling-induced vasodilation will be referred to as CIVD.

The thermoregulatory data showed that the time required to reach the core temperatures directed by the thermal protocol was associated with body mass index ($P < 0.05$), but not with body surface area or body fat percent ($P > 0.05$). Furthermore, the ΔH_b was a highly responsive variable that changed dramatically and with identical manner as soon as a participant was immersed in a different water environment. A dramatic change in ΔH_b was observed always within the first minutes of immersion in a different water tank, followed by a tendency for returning to zero. Despite these rapid changes in ΔH_b, T_{re} and T_{ty} responded with substantial delay. For instance, in Fig. 1, T_{re} remained above baseline levels for more than one-half the duration of the first cold water immersion ($t = 38$–68 min). Interestingly, it was observed that CIVD only occurred during these periods of time, that is, when ΔH_b was below zero, but T_{re} was still above baseline levels. When T_{re} reached baseline levels, or dropped below them, BF_F diminished dramatically, reaching almost zero.

Given the distinct types of warming-induced vasodilation and CIVD, HRV data were divided in those obtained during hot and cold water immersion. The χ^2 analysis showed an increased occurrence of warming- compared with cooling-induced vasodilation, and repeated-measures ANOVA detected differences in the change in T_{re} and T_f between the onset

and end of the two types of vasodilation ($P < 0.05$; Table 1). The repeated-measures ANOVA used to assess the effect of vasodilation segment (i.e., pre-CIVD, during CIVD, prewarming-induced vasodilation, during warming-induced vasodilation) on all parameters of HRV (i.e., RMSSD, pNN50, LF, HF, as well as LF/HF) demonstrated statistically significant main effects on LF, HF, and LF/HF ($P < 0.05$; Fig. 3). These effects were not attributed to changes in ventilation, since respiratory rate, ventilation, and tidal volume were found to be similar across all vasodilation segments ($P > 0.05$). Moreover, no linear relationships were detected between the HRV and the ventilatory parameters ($P > 0.05$).

Results from ROC curve analyses demonstrated that the CIVD onset cutoff points for ΔT_{re} and T_f were 0.62 and 16.76°C, respectively. Relevant univariate statistics and ROC curve analyses for the designated cutoff points appear in Table 2. Cohen's κ-statistic demonstrated significant agreement between the ΔT_{re} ($P = 0.001$) and T_f ($P < 0.001$) cutoff values and the BF_F characterization.

DISCUSSION

The present experiment provided some novel findings regarding CIVD. First, we observed two characteristic patterns of vasodilation, depending on whether participants were immersed in hot or cold water. The warming-induced vasodilation resembled a typical vasodilatory response aiming at heat dissipation (9), while the cooling-induced vasodilation demonstrated all of the characteristics that Lewis described in 1930 as CIVD (35). Thus it was assumed that the cooling-induced vasodilation observed here was CIVD. It is important to highlight that the two vasodilatory patterns occurred, despite the fact that the hand was constantly exposed to the same temperature-controlled environment, demonstrating the vast effect of core temperature on oscillations in peripheral blood flow independently of local factors.

Another interesting finding stemming from the present experiment was that CIVD occurred only during *condition B* and in times when ΔH_b was negative, but T_{re} had not yet dropped to baseline levels. Following the occurrence of all CIVD events, T_{re} was reduced, and CIVD ceased when T_{re} fell below

Table 1. *Comparisons of warming- and cooling-induced vasodilation occurrence and properties*

	Warming-Induced Vasodilation	Cooling-Induced Vasodilation
Occurrence, no.	30	16*
Duration, s	931.82±445.38	960.29±343.62
DT_{re}, °C	0.37±0.47	−0.31±0.13†
ΔBF_F, PU	192.62±186.10	39.25±50.72
ΔT_{ty}, °C	0.21±0.73	−0.28±0.36
ΔT_f, °C	4.17±8.58	−3.72±1.98†

	Pre	During	Pre	During
Ventilation, l/min	8.92±2.17	8.47±1.50	8.25±0.51	8.25±0.50
Respiratory rate, breaths/min	14.05±5.78	15.90±3.58	14.82±4.31	15.78±3.43
Tidal volume, liter	0.76±0.22	0.80±0.28	0.73±0.30	0.71±0.25

Values are means ± SD. Note: Difference (Δ) refers to the change between the onset and end of vasodilation. T_{re}, rectal temperature; BF_F, finger blood flow; PU, perfusion units; T_{ty}, tympanic temperature; T_f, finger temperature. *Significant χ^2 difference ($P < 0.05$). †Significant ANOVA difference ($P < 0.05$).
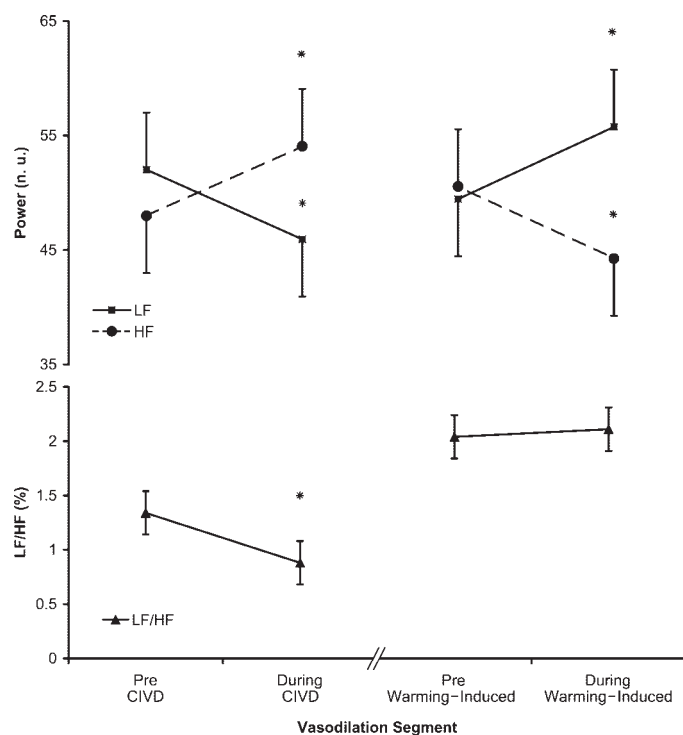
Fig. 3. Mean low- (LF) and high-frequency (HF) power spectra and mean LF-to-HF power spectra percent (LF/HF) for each vasodilation segment. Repeated-measures ANOVA demonstrated significant main effects for LF, HF, and LF/HF ($P < 0.05$). *Significant difference from previous vasodilation segment for the same vasodilation type ($P < 0.05$).

baseline. Ergo, according to the deductive reasoning rule of transposition (7), since the presence of CIVD implies excess heat in a cold environment, it can be inferred that CIVD will not occur in circumstances in which excess heat is not present in a cold environment. Additional support for this notion is provided by previous investigations in different mammalian models, suggesting a correspondence between oscillations in peripheral temperature/blood flow during cold exposures and body (8, 11, 13, 14, 17, 24, 30, 34, 37, 41, 42, 44, 46) or ambient temperature (33, 45). It is also generally agreed that there is a central component in CIVD, given that normothermic and/or centrally warm homoeotherms demonstrate accelerated CIVD responses (14, 44), while those that are centrally cold reveal CIVDs of delayed onset and lesser magnitude (14, 17, 30, 46). Ergo, there is now enough evidence to postulate that the CIVD response is triggered by excess heat with the purpose of preserving thermal balance.

The literature contains two previous studies that investigated the influence of altered thermal balance on CIVD, both showing that body heat content exerts a potent influence on CIVD (14, 43). These studies suggested that mean skin temperature and T_{re} serve as inputs for the vasomotor center in the central

nervous system that determines the finger vasomotor status by modifying the sympathetic output to the peripheral nerves (14). Based on this hypothesis, sympathetic output increases and peripheral vasoconstriction occurs when the core and the skin are cool, while CIVD appears to be superimposed on the general vascular status of the peripheral blood vessels (14). Our results are in contrast to this hypothesis, since the HRV data obtained before and during CIVD demonstrated a shift of autonomic interaction toward parasympathetic dominance. This would appear paradoxical, since it is well known that arteriovenous anastomoses [thick-walled, low-resistance blood vessels that allow high flow rates directly from arterioles to venules and play a major role in CIVD and overall thermoregulation (5, 11, 23, 24)] are innervated solely by noradrenergic sympathetic vasoconstrictor nerves (32). Hence, the fact that parasympathetic influences exceeded sympathetic effects during CIVD in our experiment is more likely due to sympathetic withdrawal than parasympathetic activation, possibly through a cholinergically induced reduction of norepinephrine released in response to sympathetic activity or a cholinergic attenuation of the response to an adrenergic stimulus (i.e., cold water immersion). It is important to mention here that the effects we observed on HRV were not attributed to changes in ventilation, since respiratory rate, ventilation, and tidal volume were found to be similar across all vasodilation segments, while no linear relationships were detected between HRV and ventilatory parameters.

Regarding the origin of the CIVD signal, our results point toward a centrally regulated mechanism (i.e., sympathetic vasoconstrictor withdrawal), in line with our previous study (19) suggesting that CIVD is the eventuality of an homoeothermic thermoregulatory function based on the suppression and activation of the sympathetic vasoconstrictor system. In his original experiment, Lewis reported absence of CIVD in fingers whose sensory nerves had been cut and had been allowed to degenerate, concluding that an axon reflex had to be the primary mechanism responsible for CIVD (35). However, others were able to obtain CIVD even after complete degeneration of the nerve supply (25). More recently, it has been also demonstrated that axon reflexes are unlikely to be the mechanism responsible for the CIVD response, since it is impossible to trigger axon reflexes in a cold hand, even when using painful electrical stimulation (12). Given that local release of vasodilator substances such as acetylcholine and histamine was not implicated in CIVD (16), it has been proposed that CIVD is caused by direct cold-induced paralysis of the peripheral blood vessels (30, 31). In our view, this hypothesis is limited in that it has been investigated only ex situ, eliminating any central influences, and it has not been confirmed in real-time CIVD data. Cold-induced paralysis of the peripheral blood vessels may well contribute to CIVD, yet our data and that of many others (8, 14, 17, 30, 34, 37, 41, 42, 46) suggest a central

Table 2. *Results for ROC curve analyses for the designated ΔT_{re} and T_f cutoff points*

	S_E (CI$_{95\%}$)	S_P (CI$_{95\%}$)	$^+$PV (CI$_{95\%}$)	$^-$PV (CI$_{95\%}$)	LR (CI$_{95\%}$)	AUC (SE)
ΔT_{re}	0.65 (0.10)	0.63 (0.12)	0.70 (0.10)	0.57 (0.12)	1.73 (0.16)	0.70 (0.03)
T_f	0.88 (0.07)	0.70 (0.11)	0.80 (0.08)	0.82 (0.10)	2.97 (0.13)	0.81 (0.09)

S_E, sensitivity; CI$_{95\%}$, 95% confidence interval; S_P, specificity; $^+$PV, positive predicted value; $^-$PV, negative predicted value; LR, likelihood ratio; AUC, area under the curve; SE, standard error.

component to CIVD. This is in line with the hypothesis that CIVD is attributed to an interruption of adrenergic neurotransmission in the cold (29). Our results support, in part, this hypothesis, since the HRV data obtained before and during CIVD suggest significant sympathetic withdrawal.

In our previous experiment (19), we proposed that CIVD is triggered by increased body heat content, and its main function is to preserve thermal balance. Indeed, in the present study, we found that the CIVD onset was 0.62°C above baseline T_{re} (ΔT_{re}), based on ROC curve analyses. This is the first study to report an objective, statistically determined ΔT_{re} cutoff point for CIVD onset. The only previous study to examine the effect of T_{re} on CIVD reported that the highest prevalence of CIVD was seen during a warm condition incorporating a ΔT_{re} of 0.2°C, compared with a nornmothermic and a cool condition (14). Based on ROC curve analysis results, the current T_f cutoff point for CIVD onset was 16.76°C. Our result is within the generally accepted temperature range of 18–15°C (5, 6, 11, 24, 26, 35), providing credence to our statistical methodology.

A logical alternative to our interpretation of the LF domain results could be the well-known baroreflex-mediated suppression of overall efferent sympathetic nervous activity during water immersion (20). However, baroreflex unloading should have occurred within the first few minutes of water immersion (20), and yet no CIVD events were observed in the first 5–10 min of immersion to a different tank. Thus we believe that our LF domain interpretation was not influenced by baroreflex activity. On the other hand, it should be noted that our results may have been influenced by participants' movement between water tanks, which generated changes in hemodynamics, possibly influencing the kinetics of the examined variables. As mean skin temperature was always "clamped" to water temperature, we did not include this parameter in our analyses. Further research on the role of vasoconstrictor nerve activity in maintaining thermal balance in homoeothermic organisms should be projected in future studies. It is concluded that CIVD is a centrally originating phenomenon caused by sympathetic vasoconstrictor withdrawal; it is dependent on body heat content, and it may be triggered by excess heat with the purpose of preserving thermal balance.

REFERENCES

1. **Akselrod S, Gordon D, Ubel FA, Shannon DC, Berger AC, Cohen RJ.** Power spectrum analysis of heart rate fluctuation: a quantitative probe of beat-to-beat cardiovascular control. *Science* 213: 220–222, 1981.
2. **[Anon].** Heart rate variability: standards of measurement, physiological interpretation and clinical use. Task Force of the European Society of Cardiology and the North American Society of Pacing and Electrophysiology. *Circulation* 93: 1043–1065, 1996.
3. **Aoyagi Y, McLellan TM, Shephard RJ.** Determination of body heat storage in clothing: calorimetry versus thermometry. *Eur J Appl Physiol* 71: 197–206, 1995.
4. **Bamber D.** The area above the ordinal dominance graph and the area below the receiver operating graph. *J Math Psychol* 12: 387–415, 1975.
5. **Bergersen TK, Eriksen M, Walloe L.** Local constriction of arteriovenous anastomoses in the cooled finger. *Am J Physiol Regul Integr Comp Physiol* 273: R880–R886, 1997.
6. **Bergersen TK, Hisdal J, Walloe L.** Perfusion of the human finger during cold-induced vasodilatation. *Am J Physiol Regul Integr Comp Physiol* 276: R731–R737, 1999.
7. **Brody BA.** Glossary of logical terms. In: *Encyclopedia of Philosophy*. London: Macmillan, 1973, p. 76.
8. **Brown RT, Baust JG.** Time course of peripheral heterothermy in a homeotherm. *Am J Physiol Regul Integr Comp Physiol* 239: R126–R129, 1980.
9. **Charkoudian N.** Skin blood flow in adult human thermoregulation: how it works, when it does not, and why. *Mayo Clin Proc* 78: 603–612, 2003.
10. **Cheung SS, Mekjavic IB.** Cold-induced vasodilatation is not homogenous or generalizable across the hand and feet. *Eur J Appl Physiol* 99: 701–705, 2007.
11. **Daanen HA.** Finger cold-induced vasodilation: a review. *Eur J Appl Physiol* 89: 411–426, 2003.
12. **Daanen HA, Ducharme MB.** Axon reflexes in human cold exposed fingers. *Eur J Appl Physiol* 81: 240–244, 2000.
13. **Daanen HA, Ducharme MB.** Finger cold-induced vasodilation during mild hypothermia, hyperthermia and at thermoneutrality. *Aviat Space Environ Med* 70: 1206–1210, 1999.
14. **Daanen HA, Van de Linde FJ, Romet TT, Ducharme MB.** The effect of body temperature on the hunting response of the middle finger skin temperature. *Eur J Appl Physiol* 76: 538–543, 1997.
15. **DuBois D, DuBois EF.** A formula to estimate the approximate surface area if height and weight be known. *Arch Intern Med* 17: 863–871, 1916.
16. **Duff F, Greenfield AD, Shepherd JT, Thompson ID, Whelan RF.** The response to vasodilator substances of the blood vessels in fingers immersed in cold water. *J Physiol* 121: 46–54, 1953.
17. **Elsner RW, Nelms JD, Irving L.** Circulation of heart to the hands of Arctic Indians. *J Appl Physiol* 15: 662–666, 1960.
18. **Fanger PO.** *Thermal Comfort: Analysis and Applications in Environmental Engineering.* Copenhagen: Danish Technical, 1970.
19. **Flouris AD, Westwood DA, Mekjavic IB, Cheung SS.** Effect of body temperature on cold induced vasodilation. *Eur J Appl Physiol* 104: 491–499, 2008.
20. **Gabrielsen A, Pump B, Bie P, Christensen NJ, Warberg J, Norsk P.** Atrial distension, haemodilution, and acute control of renin release during water immersion in humans. *Acta Physiol Scand* 174: 91–99, 2002.
21. **Gagge AP, Nishi Y.** Heat exchange between human skin surface and thermal environment. In: *Handbook of Physiology. Reactions to Environmental Agents*. Bethesda, MD: Am. Physiol. Soc., 1977, sect. 9, chapt. 5, p. 69–92.
22. **Gamelin FX, Berthoin S, Bosquet L.** Validity of the polar S810 heart rate monitor to measure R-R intervals at rest. *Med Sci Sports Exerc* 38: 887–893, 2006.
23. **Grant RT.** Observations on direct communications between arteries and veins in the rabbit's ear. *Heart* 15: 281–303, 1930.
24. **Grant RT, Bland E.** Observations on arterio-venous anastomoses in human skin and in the bird's foot with special reference to the reaction to cold. *Heart* 15: 385–411, 1931.
25. **Greenfield AD, Shepherd JT, Whelan RF.** The part played by the nervous system in the response to cold of the circulation through the finger tip. *J Physiol* 115: 10p–11p, 1951.
26. **Greenfield ADM, Shepherd JT.** A quantitative study of the response to cold of the circulation through the fingers of normal subjects. *Clin Sci* 9: 323–347, 1950.
27. **Hardy JD, DuBois EF.** The technique of measuring radiation and convection. *J Nutr* 15: 461–475, 1938.
28. **Hersen M.** *Handbook of Psychological Assessment, Case Conceptualization, and Treatment*. Hoboken, NJ: Wiley, 2007.
29. **Johnson JM, Brengelmann GL, Hales JR, Vanhoutte PM, Wenger CB.** Regulation of the cutaneous circulation. *Fed Proc* 45: 2841–2850, 1986.
30. **Keatinge WR.** The effect of general chilling on the vasodilator response to cold. *J Physiol* 139: 497–507, 1957.
31. **Keatinge WR.** Effects of temperature on blood vessels. In: *Local Mechanisms Controlling Blood Vessels*. London: Cambridge University Press, 1980, p. 99–108.
32. **Kellogg DL Jr.** In vivo mechanisms of cutaneous vasodilation and vasoconstriction in humans during thermoregulatory challenges. *J Appl Physiol* 100: 1709–1718, 2006.
33. **Kramer K, Schulze W.** Die Kältedilatation der Hautgefäße. *Pflügers Arch* 250: 141–170, 1948.

34. **Kunimoto M.** Where is the most useful point in the skin temperature curve of the fingertip immersed in the cold water to evaluate the function of the skin sympathetic function? *Biomed Thermogr* 7: 254–268, 1987.

35. **Lewis T.** Observations upon the reactions of the vessels of the human skin to cold. *Heart* 15: 177–208, 1930.

36. **Lossius K, Eriksen M, Walløe L.** Fluctuations in blood flow to acral skin in humans: connection with heart rate and blood pressure variability. *J Physiol* 460: 641–655, 1993.

37. **Meyer AA, Webster AJ.** Cold-induced vasodilatation in the sheep. *Can J Physiol Pharmacol* 49: 901–908, 1971.

38. **Minson CT, Berry LT, Joyner MJ.** Nitric oxide and neurally mediated regulation of skin blood flow during local heating. *J Appl Physiol* 91: 1619–1626, 2001.

39. **Parsons K.** *Human Thermal Environments* (3rd Ed.). London: Taylor and Francis Group, 2003.

40. **Reynolds LF, Mekjavic IB, Cheung SS.** Cold-induced vasodilatation in the foot is not homogenous or trainable over repeated cold exposure. *Eur J Appl Physiol* 102: 73–78, 2007.

41. **Sendowski I, Savourey G, Besnard Y, Bittel J.** Cold induced vasodilatation and cardiovascular responses in humans during cold water immersion of various upper limb areas. *Eur J Appl Physiol* 75: 471–477, 1997.

42. **Sendowski I, Savourey G, Launay JC, Besnard Y, Cottet-Emard JM, Pequignot JM, Bittel J.** Sympathetic stimulation induced by hand cooling alters cold-induced vasodilatation in humans. *Eur J Appl Physiol* 81: 303–309, 2000.

43. **Spealman CR.** Effect of ambient air temperature and of hand temperature on blood flow in hands. *Am J Physiol* 145: 218–222, 1945.

44. **Takano N, Kotani M.** Influence of food intake on cold-induced vasodilatation of finger. *Jpn J Physiol* 39: 755–765, 1989.

45. **Tanaka M.** Experimental studies on human reaction to cold. Differences in the vascular hunting reaction to cold according to sex, season, and environmental temperature. *Bull Tokyo Med Dent Univ* 18: 269–280, 1971.

46. **Werner J.** Influences of local and global temperature stimuli on the Lewis-reaction. *Pflügers Arch* 367: 291–294, 1977.